

## Supporting Information

# Stable silicene wrapped by graphene in air

*Yuting Nie<sup>†‡</sup>, Stepan Kashtanov<sup>†‡</sup>, Hui long Dong<sup>†</sup>, Youyong Li<sup>†</sup>, Yanyun Ma<sup>†\*</sup>, Xuhui Sun<sup>†\*</sup>*

<sup>†</sup>Institute of Functional Nano & Soft Materials (FUNSOM), Jiangsu Key Laboratory for Carbon-Based Functional Materials & Devices, Joint International Research Laboratory of Carbon-Based Functional Materials and Devices, Soochow University, 199 Ren'ai Road, Suzhou 215123, Jiangsu, P. R. China.

\* E-mail: xhsun@suda.edu.cn, mayanyun@suda.edu.cn

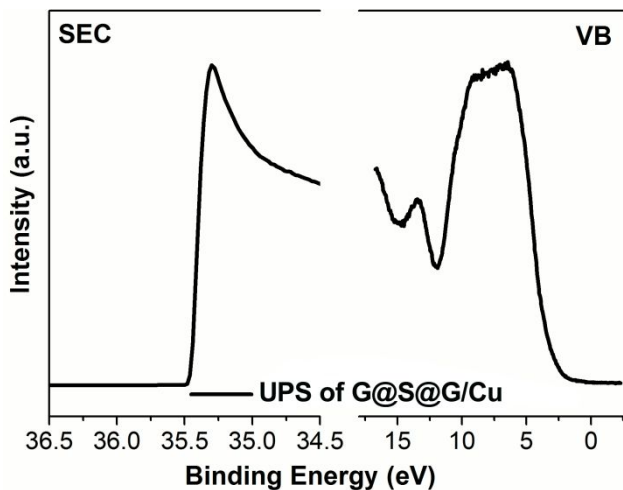


**Figure S1.** UPS spectra of G@S@G on Cu foil. Bias voltage is -5V.

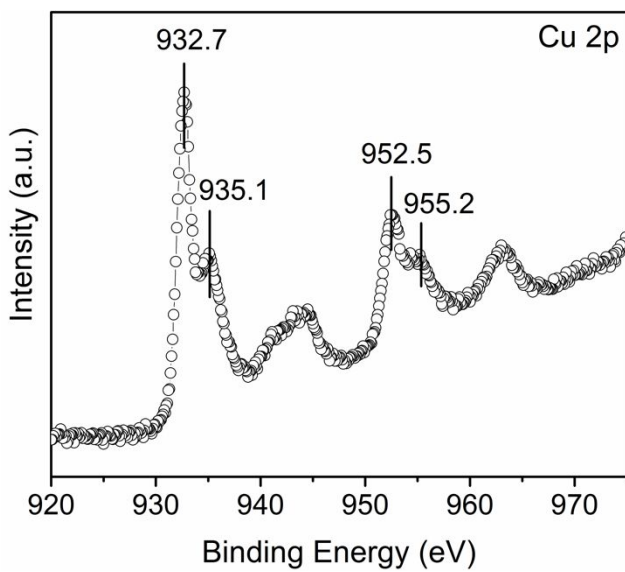


**Figure S2.** XPS spectrum of Cu 2p of G@S@G on Cu foil.

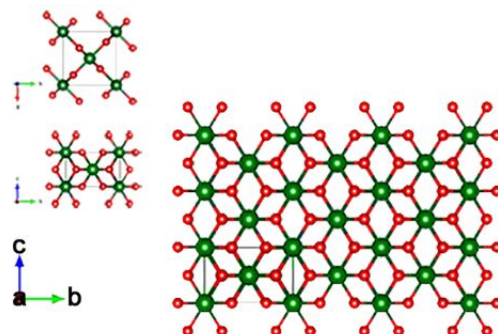


**Figure S3.** Top view, side view of unit cell and side view of 3x3x3 supercell of DFT optimized geometries of stishovite.

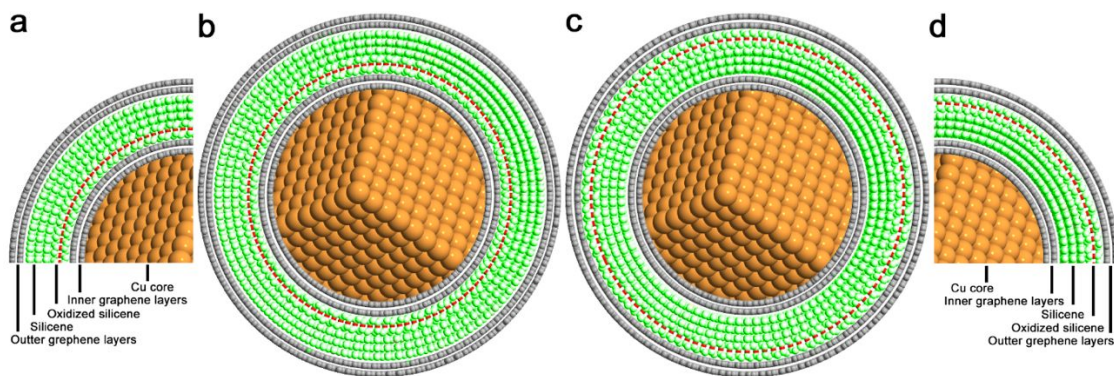


**Figure S4.** Schematic drawing of the structural composition of G@S@G with oxidized silicene in the nanosphere in two types. a) & b) oxidized silicene layer in the inner of the silicene layer, c) & d) oxidized silicene layer near outside of the silicene layer.

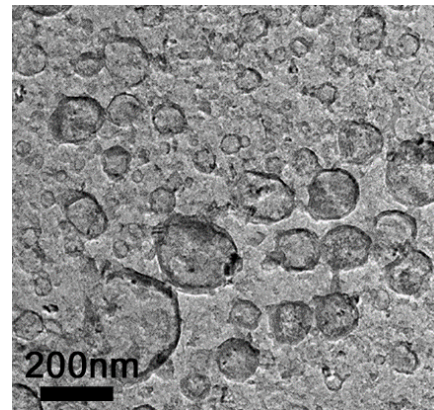


**Figure S5.** TEM image of G@S@G after Cu foil etched.

**Table S1.** The work function and interlayer distance for studied multilayer nanomaterials.

Structure	Simulation			Experiment <sup>a)</sup>		
	Work function [eV]	Dlayer [Å] (Gr-Gr)	Dlayer [Å] (Gr-Si)	Work function [eV]	Dlayer [Å] (Gr-Gr)	Dlayer [Å] (Gr-Si)
BLG	4.52	3.35		4.65-4.75	3.4	
Gr+silicene	4.66		3.53			
BLG/silicene	4.93	3.35	3.05			
BLG/Silic-1O	5.04	4.91	3.52			
BLG/Silic-2O	4.50	3.83	3.92			
BLG/stishovite	5.37	4.04	4.05			

a) Experimentally measured values from references.<sup>1-2</sup>

## Note 1

**Work function and distance between the layers.** Calculated values of distance between layers, work function are simulated with performed by CASTEP program.<sup>3</sup> GGA-PBE is used to describe the electronic exchange and correlation interaction.<sup>4</sup> The dispersion interactions are considered using the semi-empirical scheme proposed by Grimme.<sup>5</sup> Ultra-soft pseudo-potential is adopted with the plane-wave cutoff energy of 300 eV. Different k-points are employed to different bilayer nanomaterials. Bilayer graphene (BLG) is also used for comparison by applying a Monkhorst-Pack grid of  $12 \times 12 \times 1$  for geometry optimization and  $20 \times 20 \times 1$  for electronic property calculations,<sup>6</sup> which shows good accordance with the experimentally measured values.<sup>2</sup> Calculated values of distance between layers, work function are shown in Table S1.

**Table S2.** Cell parameters, crystallographic data and chemical bond parameters for optimized structures

Silicene-ML				Silic-1O				Silic-2O								
Cell			Cell			Cell			Cell							
Length	a [Å]	b [Å]	c [Å]	Length	a [Å]	b [Å]	c [Å]	Length	a [Å]	b [Å]	c [Å]					
	3.8785	3.8784	3.5062		3.9250	3.9248	4.6846		4.0699	3.9465	4.6996					
Angle	$\alpha$	$\beta$	$\gamma$	Angle	$\alpha$	$\beta$	$\gamma$	Angle	$\alpha$	$\beta$	$\gamma$					
	89.99	90.00	120.00		114.78	65.22	120.02		104.51	81.29	120.75					
Atom	frac. x	frac. y	frac. z	Atom	frac. x	frac. y	frac. z	Atom	frac. x	frac. y	frac. z					
Si	0.3501	0.1992	0.5858	Si	0.4849	0.1454	0.9519	Si	0.2197	0.3181	0.2794					
Si	0.6834	0.8659	0.4142	Si	0.7576	0.8727	0.1337	Si	0.5541	0.0353	0.4176					
				O	0.6166	0.0158	0.5428	O	0.5805	0.1898	0.7970					
								O	0.1942	0.1666	0.9000					
Si-Si				Si-Si		Si-O		Si-Si		Si-O						
Bond length	2.32 Å			Bond length	2.38 Å		1.68 Å		Bond length	2.38 Å		1.74 Å				
Si-Si-Si				Si-Si-Si				Si-Si-Si			Si-O-O					
Bond angle	113.5°			Bond angle	110.71°				Bond angle	111.97°			104.88°			
Bulking distance	0.6 Å			Bulking distance	0.745 Å				Bulking distance	0.62 Å						

## Note 2

**Crystal structure optimization, stacked interactions.** First-principles ab-initio approach was utilized in the framework of DFT within the Perdew-Burke-Ernzerhof (PBE) generalized gradient approximation (GGA).<sup>4, 7-10</sup> The cutoff energy of 320 eV was used for the plane-wave expansion of wave functions.<sup>11-13</sup> A scheme by Monkhorst and Pack was carried out for k-point sampling of Brillouin zone.<sup>6, 11-13</sup> The grid was set as follows depending on the specific geometry: monolayer, 2D cell optimization with k-grid 13x13x1; bulk, unit cell optimization: k-grid 9x9x10, 41x41x11; bulk, super cell, cell optimization, k-grid: 3x3x3, 9x9x9. All the unit cells were fully relaxed with

no constraints until the corresponding energy and forces had been converged to  $10^{-5}$  eV and 0.01 eV/Å, respectively. Long range vdW interactions in stacking geometries were accounted by employing both Grimme and other nonempirical vdW corrections to GGA.<sup>5, 14-19</sup> Calculations were performed with Quantum Espresso and CASTEP software packages.<sup>3, 20</sup> Optimized unit cell parameters and fractional coordinates for all these structures are listed in Table S2.

Simulated structure of multilayered silicene (named as Silicene-ML) consists of stacked layers of silicene sheets. Each layer is exactly on top of the other. Unit cell of this structure contains two Si atoms. Top view reveals a honeycomb arrangement of Si atomic centers. From the 2D perspective, the Silicene-ML is very similar to the structure of conventional 2D silicene sheet with lattice parameter 3.87 Å. The Si–Si bond length is 2.32 Å and Si–Si–Si bond angle is 113.5°. These result in a buckling distance of 0.6 Å. In case of true 2D silicene it is 0.47 Å, hence the deviations are quite small. The simulated structure of Silicene-ML is shown in Figure 2e inset.

Structure Silic-1O with single oxygen atom per unit cell also exhibit a layered visual appearance when being viewed from the side. Despite on that, the layers of silicon atoms here are not the same as that in silicene. Unit cell vectors for this configuration show significant distortions from the ones for multilayered silicene. In Silic-1O structure, each layer contains Si atoms in tetrahedral spatial arrangement. Oxygen atoms are acting as bridges interconnecting such layers by forming atomic bond with Si atoms from two adjacent layers simultaneously. Each Si atom possesses tetrahedral bonding arrangement with three Si and one O neighboring atoms. Distance between Si atoms (Si–Si) is 2.38 (Å) and Si–O bond length is 1.68 Å. The simulated structure of Silic-1O is shown in Figure 2e inset.

In the Silic-2O structure, the layers of Si atoms are indeed resembling the honeycomb structure of silicene. Unit cell parameters of Silic-2O in the a-b plane are just slightly off the values that

corresponds to the 2D silicene sheet. Each unit cell contain two Si atoms accompanied with two O atoms. Super cell view of this configuration show that layers of Si atoms are slightly shifted with respect to each other. Oxygen molecules act as bridges connecting these layers. The Si–Si bond length is 2.38 Å which is similar to the one in Silic-1O. The Si–Si–Si bond angle is 111.97° in Silic-2O but 110.71° in Silic-1O. The Si–O bond length is 1.74 Å and Si–O–O angle is 104.88°. Therefore, buckling of Si atoms in Silic-2O is 0.62 Å, which is again quite close to the buckling in 2D silicene. The simulated structure of Silic-2O is shown in Figure 2e inset.

**Table S3.** Si K-edge ionization potential (IP) and  $\sigma \rightarrow \pi^*$  photon energy values.

Model	Structure		Simulation <sup>a)</sup>		Experiments		Simulation (corrected) <sup>f)</sup>	
			IP	$\sigma \rightarrow \pi^*$	IP	$\sigma \rightarrow \pi^*$	IP	$\sigma \rightarrow \pi^*$
		(eV)	(eV) <sup>b)</sup>	(eV)	(eV)	(eV)	(eV)	(eV)
Silicene-ML	1852.1 2	1848.8 0		1848.8 (D) <sup>c)</sup>	1841.1 (A) <sup>c)</sup>		1848.10 (- 3.3)	1841.10 (- 7.7)
Silic-1O	1853.6 0	1849.5 0		1848.8 (D) <sup>c)</sup>	1846.2 (C) <sup>c)</sup>		1849.00 <sup>g)</sup>	1843.00 <sup>g)</sup>
Silic-2O	1853.7 0	1848.2 0		1848.8 (D) <sup>c)</sup>	1843.6 (B) <sup>c)</sup>		1849.10 <sup>g)</sup>	1841.70 <sup>g)</sup>
Stishovite	1855.6 0	1852.5 0		1851.0 <sup>d)</sup>	1846.0 <sup>d)</sup>		1851.00 (- 4.6)	1846.00 (- 6.5)
Silicon	1852.0 3	1848.8 0		1848.0 <sup>e)</sup>	1840.0 <sup>e)</sup>		1848.00 (- 4.0)	1840.00 (- 8.8)
$\alpha$ -Quartz	1856.0 0	1854.0 0		1849.0 <sup>e)</sup>	1845.0 <sup>e)</sup>		1849.00 (- 7.0)	1845.00 (- 9.0)

a) Value obtained with half-core approximation. b) As seen in convoluted simulated absorption profile. c) Experimentally measured values from this work. d) Experimentally measured values from references.<sup>21-22</sup> e) Experimentally measured values from references.<sup>23-24</sup> f) Corrections as difference between simulation and experimental values are shown in the brackets. g) Same corrections as for stishovite.

### Note 3

**Oscillator strengths for absorption transitions and X-ray absorption near-edge spectra (XANES).** Quantum chemical calculations have been performed to assign the observed peaks in the experimental X-ray absorption spectra. XANES spectra were computed at the GGA DFT level using STOBE-DEMON numerical package with the gradient corrected Becke exchange functional and the Perdew correlation functional.<sup>25-28</sup> Oscillator strengths of transitions were computed for both half-core-hole and full-core-hole approximations by the transition potential (TP) method in combination with a double basis set technique followed by Delta Kohn–Sham (DKS) scheme.<sup>29-32</sup> In order to obtain an improved representation of relaxation effects in the inner orbitals, the ionized atomic center was described by the IGLO-III basis of Kutzelnig and effective core potentials (ECP) were used on all other atoms.<sup>33-34</sup> To mimic the experimental broadening of the experimental spectra, all simulated electronic transitions were then subjected to Gaussian convolution with varying broadening. For the region below the ionization threshold the broadening [full width at half maximum (FWHM)] was set to 1.5 eV. Above the threshold the constant broadening of 4.5 eV was applied. Si K-edge ionization potential (IP) and  $\sigma \rightarrow \pi^*$  photon energy values are shown in Table S3.

**Table S4.** Simulated Si 2p and O 1s core-electron binding energy values with and without correction for selected model structures.

Structure	Bonding	Binding energy (eV)			
		Without correction		With correction	
		Si 2p	O 1s	Si 2p	O 1s
Silic-2O	Si-O2-Si	103.18	530.94	102.23	533.44
Silic-1O	Si-O-Si	102.66	528.73	101.71	531.23
$\alpha$ -quartz	Si-O4	104.19	529.82	103.89	532.70

Stishovite	Si-O8	103.10	528.21	102.80	531.09
Silicene-ML	Si-Si	101.22		98.29	

**Table S5.** Simulated Si 2p, O 1s, C 1s core-electron binding energy values for selected model structures.

Molecule	Simulated binding energy (eV) <sup>a)</sup>				
	Si	O1	O2	C1	C2
ATOTMS	102.62	530.20	529.29	288.04	
VTETOS	103.10	529.59			
DMOMS <sup>b)</sup>	102.74	529.50			
PHS	102.40			284.04(sp <sup>2</sup> )	284.33
HMDSO		528.86		284.03(sp <sup>3</sup> )	284.20
PS	102.28				
HMDS	101.39				
PDMS	101.16				

a) with PBE/TZP, b) for DMOMS/PDMSO.

**Table S6.** Corrections to simulated Si 2p core-electron binding energy values for different bonding environments

Method	Bonding arrangement (Model)					
	In-plane (PDMS)	Si-Si	Spatial (Silicon)	Si-Si	In-plane (DMOMS) <sup>b)</sup>	Spatial Si-O ( $\alpha$ -Quartz)
PBE/tzp	101.16		102.04		102.74	104.18
Exp. <sup>a)</sup>	98.1		99.1		101.79	103.7
err.	-3.06		-2.94		-0.95	-0.48

a) see references<sup>35-40</sup> b) for DMOMS/PDMSO.

**Table S7.** Corrections to simulated C 1s core-electron binding energy values for different bonding environments

Method	Bonding arrangement (Model)			
	Si-Si-C (PDMS)	O-Si-C (DMOMS) <sup>b)</sup>	C(sp <sup>2</sup> ) (PHS)	C=O (ATOTM)
PBE/tzp	283.52	283.84	284.33	288.04
Exp. <sup>a)</sup>	283.5	284.38	284.47	288.2
err.	-0.02	0.54	0.14	0.16

a) see references,<sup>35-39, 41-43</sup> b) for DMOMS/PDMSO

**Table S8.** Corrections to simulated O 1s core-electron binding energy values for different bonding environments

Method	Bonding arrangement (Model)	
	n-plane Si-O (DMOMS) <sup>b)</sup>	Spatial Si-O ( $\alpha$ -Quartz)
PBE/tzp	529.50	529.82
Exp. <sup>a)</sup>	532.00	532.70
err.	2.50	2.88

a) see references,<sup>35, 44-46</sup> b) for DMOMS/PDMSO

**Table S9** Si 2p, O 1s, C 1s core-electron binding energies for selected small molecules and different bonding environments.

Molecule	Bonding	Simulation			Experiment <sup>a)</sup>		
		Si 2p (eV)	O 1s (eV)	C 1s (eV)	Si 2p (eV)	O 1s (eV)	C 1s (eV)
Silane	Si-H	106.80					

For. acid	C=O	537.96		538.97	
For. acid	C-OH	539.70		540.63	
Water	H-O	538.97		539.90	
CO <sub>2</sub>	C=O	540.33	296.70	541.28	297.69
CO	C=O	541.60	295.70	542.55	296.21
Ethene	C=C		290.26		283.60
Methanol	C-OH	537.70	291.50	539.11	
Acetone	C=O	536.44	290.80		
Ether	C-O	536.71	289.66		

a) see references.<sup>35-46</sup>

**Table S10** Simulated Si 2p core-electron binding energy values with and without correction.

Method	With corrections applied				
	Bonding arrangement		DBE (eV)	Bonding arrangement	
	Si-O-C	O-Si-O		Si-O-C	O-Si-O
	ATOTMS	DMOMS		ATOTMS	DMOMS
BLYP/tzp	102.80	102.93	-0.13	101.85	101.98
OLYP/tzp	103.13	103.26	-0.13	102.18	102.31
PBE/tzp	102.62	102.74	-0.12	101.67	101.79
PW91/tzp	102.84	102.97	-0.12	101.89	102.02
BLYP/aug-tzp	102.79	102.92	-0.12	101.84	101.97
OLYP/aug-tzp	103.12	103.24	-0.12	102.17	102.29
PBE/aug-tzp	102.61	102.72	-0.11	101.66	101.77
PW91/aug-tzp	102.83	102.95	-0.11	101.88	102.00
	Si-O <sub>3</sub>	O-Si-O			
	VTETOS	DMOMS			
BLYP/tzp	102.80	102.93	-0.13	102.32	101.98
OLYP/tzp	103.13	103.26	-0.13	102.65	102.31

PBE/tzp	102.62	102.74	-0.12	102.14	101.79
PW91/tzp	102.84	102.97	-0.12	102.36	102.02
BLYP/aug-tzp	102.79	102.92	-0.12	102.31	101.97
OLYP/aug-tzp	103.12	103.24	-0.12	102.64	102.29
PBE/aug-tzp	102.61	102.72	-0.11	102.13	101.77
PW91/aug-tzp	102.83	102.95	-0.11	102.35	102.00
	Si-O4	O-Si-O			
	$\alpha$ -Quartz	DMOMS			
BLYP/tzp	104.39	102.93	1.46	103.91	101.98
OLYP/tzp	104.74	103.26	1.48	104.26	102.31
PBE/tzp	104.19	102.74	1.44	103.71	101.79
PW91/tzp	104.41	102.97	1.44	103.93	102.02
BLYP/aug-tzp	104.62	102.92	1.71	104.14	101.97
OLYP/aug-tzp	104.94	103.24	1.70	104.46	102.29
PBE/aug-tzp	104.40	102.72	1.68	103.92	101.77
PW91/aug-tzp	104.63	102.95	1.68	104.15	102.00
	Si-Si	O-Si-O			
	Silicene	DMOMS			
BLYP/tzp	101.95	102.93	-0.98	99.01	101.98
OLYP/tzp	102.51	103.26	-0.75	99.58	102.31
PBE/tzp	102.04	102.74	-0.70	99.10	101.79
PW91/tzp	102.21	102.97	-0.76	99.27	102.02
BLYP/aug-tzp	101.94	102.92	-0.98	99.00	101.97
OLYP/aug-tzp	102.50	103.24	-0.74	99.56	102.29
PBE/aug-tzp	102.02	102.72	-0.70	99.09	101.77
PW91/aug-tzp	102.19	102.95	-0.75	99.26	102.00
	Si-Si	O-Si-O			
	Silicene 3D	DMOMS			
BLYP/tzp	101.96	102.93	-0.97	99.02	101.98

OLYP/tzp	102.53	103.26	-0.73	99.59	102.31
PBE/tzp	102.05	102.74	-0.69	99.11	101.79
PW91/tzp	102.22	102.97	-0.75	99.28	102.02
BLYP/aug-tzp	101.95	102.92	-0.96	99.01	101.97
OLYP/aug-tzp	102.52	103.24	-0.72	99.58	102.29
PBE/aug-tzp	102.03	102.72	-0.69	99.10	101.77
PW91/aug-tzp	102.21	102.95	-0.74	99.27	102.00
	Si-Si	O-Si-O			
	Silicene ML	DMOMS			
BLYP/tzp	101.32	102.93	-1.62	98.38	101.98
OLYP/tzp	101.72	103.26	-1.54	98.78	102.31
PBE/tzp	101.22	102.74	-1.52	98.29	101.79
PW91/tzp	101.50	102.97	-1.46	98.57	102.02
BLYP/aug-tzp	101.45	102.92	-1.46	98.51	101.97
OLYP/aug-tzp	101.72	103.24	-1.52	98.78	102.29
PBE/aug-tzp	101.34	102.72	-1.39	98.40	101.77
PW91/aug-tzp	102.07	102.95	-0.87	99.14	102.00
	O-Si-O	O-Si-O			
	Sili w1O	DMOMS			
BLYP/tzp	102.65	102.93	-0.28	101.70	101.98
OLYP/tzp	103.16	103.26	-0.10	102.21	102.31
PBE/tzp	102.66	102.74	-0.08	101.71	101.79
PW91/tzp	102.85	102.97	-0.12	101.90	102.02
BLYP/aug-tzp	102.68	102.92	-0.24	101.73	101.97
OLYP/aug-tzp	103.18	103.24	-0.05	102.23	102.29
PBE/aug-tzp	102.68	102.72	-0.04	101.73	101.77
PW91/aug-tzp	102.87	102.95	-0.08	101.92	102.00
	O2-Si-O2	O-Si-O			
	Sili w1O	DMOMS			

BLYP/tzp	103.15	102.93	0.22	102.20	101.98
OLYP/tzp	103.70	103.26	0.44	102.75	102.31
PBE/tzp	103.18	102.74	0.44	102.23	101.79
PW91/tzp	103.37	102.97	0.40	102.42	102.02
BLYP/aug-tzp	103.18	102.92	0.27	102.23	101.97
OLYP/aug-tzp	103.72	103.24	0.48	102.77	102.29
PBE/aug-tzp	103.21	102.72	0.48	102.26	101.77
PW91/aug-tzp	103.40	102.95	0.45	102.45	102.00
	Si-O <sub>8</sub>	O-Si-O			
	stishovite	DMOMS			
BLYP/tzp	104.30	102.93	1.36	103.82	101.98
OLYP/tzp	103.76	103.26	0.50	103.28	102.31
PBE/tzp	103.10	102.74	0.36	102.62	101.79
PW91/tzp	103.31	102.97	0.34	102.83	102.02
BLYP/aug-tzp	103.73	102.92	0.81	103.25	101.97
OLYP/aug-tzp	103.71	103.24	0.47	103.23	102.29
PBE/aug-tzp	103.49	102.72	0.76	103.01	101.77
PW91/aug-tzp	103.49	102.95	0.55	103.01	102.00

**Table S11** Simulated O 1s core-electron binding energy values with and without correction.

Method	With corrections applied				
	Bonding arrangement		DBE (eV)	Bonding arrangement	
	Si-O <sub>3</sub>	O-Si-O		Si-O <sub>3</sub>	O-Si-O
	VTETOS	DMOMS		VTETOS	DMOMS
BLYP/tzp	530.04	529.96	0.08	530.04	532.46
OLYP/tzp	529.25	529.17	0.07	529.25	531.67
PBE/tzp	529.59	529.50	0.09	529.59	532.00
PW91/tzp	529.96	529.88	0.09	529.96	532.38

BLYP/aug-tzp	530.03	529.96	0.08	530.03	532.46
OLYP/aug-tzp	529.24	529.17	0.07	529.24	531.67
PBE/aug-tzp	529.58	529.50	0.08	529.58	532.00
PW91/aug-tzp	529.95	529.87	0.08	529.95	532.37

	Si-O-C	O-Si-O		Si-O-C	O-Si-O
	ATOTMS	DMOMS		ATOTMS	DMOMS
BLYP/tzp	530.71	529.96	0.75	533.21	532.46
OLYP/tzp	529.85	529.17	0.67	532.35	531.67
PBE/tzp	530.20	529.50	0.70	532.70	532.00
PW91/tzp	530.59	529.88	0.71	533.09	532.38
BLYP/aug-tzp	530.71	529.96	0.75	533.21	532.46
OLYP/aug-tzp	529.84	529.17	0.67	532.34	531.67
PBE/aug-tzp	530.19	529.50	0.70	532.69	532.00
PW91/aug-tzp	530.58	529.87	0.71	533.08	532.37
	Si-O-Si	O-Si-O		Si-O-Si	O-Si-O
	DMS	DMOMS		DMS	DMOMS
BLYP/tzp	529.37	529.96	-0.60	531.87	532.46
OLYP/tzp	528.47	529.17	-0.71	530.97	531.67
PBE/tzp	528.86	529.50	-0.64	531.36	532.00
PW91/tzp	529.25	529.88	-0.63	531.75	532.38
BLYP/aug-tzp	529.35	529.96	-0.61	531.85	532.46
OLYP/aug-tzp	528.46	529.17	-0.71	530.96	531.67
PBE/aug-tzp	528.85	529.50	-0.65	531.35	532.00
PW91/aug-tzp	529.23	529.87	-0.64	531.73	532.37
	Si-O4	O-Si-O		Si-O4	O-Si-O
	$\alpha$ -quartz	DMOMS		$\alpha$ -quartz	DMOMS
BLYP/tzp	530.30	529.96	0.33	533.18	532.46
OLYP/tzp	529.44	529.17	0.27	532.32	531.67
PBE/tzp	529.82	529.50	0.31	532.70	532.00

PW91/tzp	530.20	529.88	0.32	533.08	532.38
BLYP/aug-tzp	530.32	529.96	0.36	533.20	532.46
OLYP/aug-tzp	529.49	529.17	0.32	532.37	531.67
PBE/aug-tzp	529.85	529.50	0.35	532.73	532.00
PW91/aug-tzp	530.23	529.87	0.36	533.11	532.37

	Si-O8	O-Si-O		Si-O8	O-Si-O
	Stishovite	DMOMS		Stishovite	DMOMS
BLYP/tzp	528.67	529.96	-1.29	531.56	532.46
OLYP/tzp	527.85	529.17	-1.33	530.73	531.67
PBE/tzp	528.21	529.50	-1.30	531.09	532.00
PW91/tzp	528.58	529.88	-1.30	531.46	532.38
BLYP/aug-tzp	528.64	529.96	-1.32	531.52	532.46
OLYP/aug-tzp	527.83	529.17	-1.34	530.71	531.67
PBE/aug-tzp	528.18	529.50	-1.32	531.06	532.00
PW91/aug-tzp	528.55	529.87	-1.32	531.43	532.37

	Si-O-Si	O-Si-O		Si-O-Si	O-Si-O
	Sili w1O	DMOMS		Sili w1O	DMOMS
BLYP/tzp	529.17	529.96	-0.79	531.67	532.46
OLYP/tzp	528.34	529.17	-0.83	530.84	531.67
PBE/tzp	528.73	529.50	-0.77	531.23	532.00
PW91/tzp	529.10	529.88	-0.78	531.60	532.38
BLYP/aug-tzp	529.19	529.96	-0.77	531.69	532.46
OLYP/aug-tzp	528.37	529.17	-0.80	530.87	531.67
PBE/aug-tzp	528.75	529.50	-0.75	531.25	532.00
PW91/aug-tzp	529.12	529.87	-0.75	531.62	532.37

	Si-O2-Si	O-Si-O		Si-O2-Si	O-Si-O
	Sili w2O	DMOMS		Sili w2O	DMOMS
BLYP/tzp	531.39	529.96	1.42	533.89	532.46
OLYP/tzp	530.65	529.17	1.48	533.15	531.67

PBE/tzp	530.94	529.50	1.44	533.44	532.00
PW91/tzp	531.31	529.88	1.44	533.81	532.38
BLYP/aug-tzp	531.37	529.96	1.41	533.87	532.46
OLYP/aug-tzp	530.64	529.17	1.47	533.14	531.67
PBE/aug-tzp	530.93	529.50	1.43	533.43	532.00
PW91/aug-tzp	531.30	529.87	1.43	533.80	532.37

#### Note 4

**Core-electron ionization potentials (core-electron binding energies).** The core-electron ionization potentials were calculated in the  $\Delta$ KS (Kohn–Sham) scheme in which the energy is taken as the difference between the optimized ground state and core-ionized state. To be able to compare with experimental data the 1s core state was considered for oxygen and carbon elements, whereas 2p core state was considered for silicon. Gradient-corrected functional with both polarized triple-zeta (TZP) and augmented polarized triple-zeta (aug-TZP) basis sets were used in the calculations. Calculations were performed in ADF program suite.<sup>26, 47-53</sup> The core-electron ionization potentials of the Si, C, O are shown in Table S4-11.<sup>53</sup>

#### REFERENCES

1. Spencer, M. J. S.; Morishita, T., *Silicene-Structure, Properties and Applications*. Springer: Springer International Publishing Switzerland 2016; Vol. 235, p 283.
2. Yu, Y. J.; Zhao, Y.; Ryu, S.; Brus, L. E.; Kim, K. S.; Kim, P., Tuning the Graphene Work Function by Electric Field Effect. *Nano Lett.* **2009**, 9 (10), 3430-3434.
3. Clark, S. J.; Segall, M. D.; Pickard, C. J.; Hasnip, P. J.; Probert, M. I.; Refson, K.; Payne, M. C., First Principles Methods Using Castep. *Z. Kristallogr* **2005**, 220 (5/6), 567.
4. Perdew, J. P.; Burke, K.; Ernzerhof, M., Generalized Gradient Approximation Made Simple. *Phys. Rev. Lett.* **1996**, 77 (18), 3865.

5. Grimme, S., Semiempirical Gga-Type Density Functional Constructed with a Long-Range Dispersion Correction. *J. Comput. Chem.* **2006**, 27 (15), 1787-1799.
6. Monkhorst, H. J.; Pack, J. D., Special Points for Brillouin-Zone Integrations. *Phys. Rev. B* **1976**, 13 (12), 5188-5192.
7. Hohenberg, P.; Kohn, W., Inhomogeneous Electron Gas. *Phys. Rev.* **1964**, 136 (3B), B864-B871.
8. Kohn, W.; Sham, L. J., Self-Consistent Equations Including Exchange and Correlation Effects. *Phys. Rev.* **1965**, 140 (4A), A1133-A1138.
9. Calais, J. L., Density-Functional Theory of Atoms and Molecules. In *Int. J. Quantum Chem.*, R.G. Parr and W. Yang, Ed. Oxford University Press, : New York, Oxford, 1989. IX + 333 pp., 1993; Vol. 47, pp 101.
10. Becke, A. D., The Challenge of D and F Electrons: Theory and Computation. In *American Chemical Society*, Salahub, D. R.; Zerner, M. C., Eds. Washington, DC, 1989; Vol. 394, pp 165-179.
11. Vanderbilt, D., Soft Self-Consistent Pseudopotentials in a Generalized Eigenvalue Formalism. *Phys. Rev. B* **1990**, 41 (11), 7892-7895.
12. Blöchl, P. E., Projector Augmented-Wave Method. *Phys. Rev. B* **1994**, 50 (24), 17953-17979.
13. Wright, A. F., Elastic Properties of Zinc-Blende and Wurtzite Aln, Gan, and Inn. *J. Appl. Phys.* **1997**, 82 (6), 2833-2839.
14. Dion, M.; Rydberg, H.; Schröder, E.; Langreth, D. C.; Lundqvist, B. I., Van Der Waals Density Functional for General Geometries. *Phys. Rev. Lett.* **2004**, 92 (24), 246401.
15. Tkatchenko, A.; Scheffler, M., Accurate Molecular Van Der Waals Interactions from Ground-State Electron Density and Free-Atom Reference Data. *Phys. Rev. Lett.* **2009**, 102 (7), 073005.
16. Grimme, S.; Mück-Lichtenfeld, C.; Antony, J., Noncovalent Interactions between Graphene Sheets and in Multishell (Hyper)Fullerenes. *J. Phys. Chem. C* **2007**, 111 (30), 11199-11207.
17. Di Leva, A.; Gialanella, L.; Kunz, R.; Rogalla, D.; Schürmann, D.; Strieder, F.; De Cesare, M.; De Cesare, N.; D'Onofrio, A.; Fülöp, Z.; Gyürky, G.; Imbriani, G.; Mangano, G.; Ordine, A.; Roca, V.; Rolfs, C.; Romano, M.; Somorjai, E.; Terrasi, F., Stellar and Primordial Nucleosynthesis of  $^7\text{Be}$ : Measurement of  $^3\text{He}$  ( $\alpha$ ,  $\gamma$ )  $^7\text{Be}$ . *Phys. Rev. Lett.* **2009**, 102 (23), 232502.
18. Klimeš, J.; Bowler, D. R.; Michaelides, A., Van Der Waals Density Functionals Applied to Solids. *Phys. Rev. B* **2011**, 83 (19), 195131.
19. Moellmann, J.; Grimme, S., DFT-D3 Study of Some Molecular Crystals. *J. Phys. Chem. C* **2014**, 118 (14), 7615-7621.

20. Giannozzi, P.; Baroni, S.; Bonini, N.; Calandra, M.; Car, R.; Cavazzoni, C.; Ceresoli, D.; Chiarotti, G. L.; Cococcioni, M.; Dabo, I.; Dal Corso, A.; de Gironcoli, S.; Fabris, S.; Fratesi, G.; Gebauer, R.; Gerstmann, U.; Gougaussis, C.; Kokalj, A.; Lazzeri, M.; Martin-Samos, L.; Marzari, N.; Mauri, F.; Mazzarello, R.; Paolini, S.; Pasquarello, A.; Paulatto, L.; Sbraccia, C.; Scandolo, S.; Sclauzero, G.; Seitsonen, A. P.; Smogunov, A.; Umari, P.; Wentzcovitch, R. M., Quantum Espresso: A Modular and Open-Source Software Project for Quantum Simulations of Materials. *J. Phys.: Condens. Matter* **2009**, 21 (39), 395502.
21. Li, D.; Bancroft, G. M.; Kasrai, M.; Fleet, M. E.; Feng, X. H.; Tan, K. H.; Yang, B. X., High-Resolution Si K- and L<sub>2,3</sub>-Edge XANES of  $\alpha$ -Quartz and Stishovite. *Solid State Commun.* **1993**, 87 (7), 613-617.
22. Nishiyama, N.; Wakai, F.; Ohfuchi, H.; Tamenori, Y.; Murata, H.; Taniguchi, T.; Matsushita, M.; Takahashi, M.; Kulik, E.; Yoshida, K.; Wada, K.; Bednarcik, J.; Irifune, T., Fracture-Induced Amorphization of Polycrystalline SiO<sub>2</sub> Stishovite: A Potential Platform for Toughening in Ceramics. *Sci. Rep.* **2014**, 4 (1), 6558.
23. Sammynaiken, R.; Naftel, S. J.; Sham, T. K.; Cheah, K. W.; Averboukh, B.; Huber, R.; Shen, Y. R.; Qin, G. G.; Ma, Z. C.; Zong, W. H. Z., Structure and Electronic Properties of SiO<sub>2</sub>/Si Multilayer Superlattices: Si K Edge and L<sub>3,2</sub> Edge X-Ray Absorption Fine Structure Study. *J. Appl. Phys.* **2002**, 92 (6), 3000-3006.
24. Zhong, J.; Zhang, H.; Sun, X.; Lee, S. T., Synchrotron Soft X-Ray Absorption Spectroscopy Study of Carbon and Silicon Nanostructures for Energy Applications. *Adv. Mater.* **2014**, 26 (46), 7786-7806.
25. Perdew, J. P., Density-Functional Approximation for the Correlation Energy of the Inhomogeneous Electron Gas. *Phys. Rev. B* **1986**, 33 (12), 8822-8824.
26. Becke, A. D., Density-Functional Exchange-Energy Approximation with Correct Asymptotic Behavior. *Phys. Rev. A* **1988**, 38 (6), 3098-3100.
27. Hermann, K.; Pettersson, L. G. M.; Casida, M. E.; Daul, C.; Goursot, A.; Koester, A.; Proynov, E.; St-Amant, A.; Salahub, D. R.; Carravetta, V.; Duarte, H.; Godbout, N.; Guan, J.; Jamorski, C.; Leboeuf, M.; Malkin, V.; Malkina, O.; Nyberg, M.; Pedocchi, L.; Sim, F.; Triguero, L.; Vela, A.; *StoBe-deMon Version 1.0*. Berlin: 2002.
28. Stöhr, J., *Nexafs Spectroscopy*. Springer: Berlin ; New York, 1996; p 403.
29. Ågren, H.; Carravetta, V.; Vahtras, O.; Pettersson, L. G. M., Direct Scf Direct Static-Exchange Calculations of Electronic Spectra. *Theor. Chem. Acc.* **1997**, 97 (1), 14-40.
30. Kolczewski, C.; Püttner, R.; Plashkevych, O.; Ågren, H.; Staemmler, V.; Martins, M.; Snell, G.; Schlachter, A. S.;

- Sant'Anna, M.; Kaindl, G.; Pettersson, L. G. M., Detailed Study of Pyridine at the C 1s and N 1s Ionization Thresholds: The Influence of the Vibrational Fine Structure. *J. Chem. Phys.* **2001**, 115 (14), 6426-6437.
31. Triguero, L.; Pettersson, L. G. M.; Ågren, H., Calculations of Near-Edge X-Ray-Absorption Spectra of Gas-Phase and Chemisorbed Molecules by Means of Density-Functional and Transition-Potential Theory. *Phys. Rev. B* **1998**, 58 (12), 8097-8110.
  32. Cavalleri, M.; Odelius, M.; Nordlund, D.; Nilsson, A.; Pettersson, L. G. M., Half or Full Core Hole in Density Functional Theory X-Ray Absorption Spectrum Calculations of Water? *Phys. Chem. Chem. Phys.* **2005**, 7 (15), 2854-2858.
  33. Fleischer, U.; Kutzelnigg, W.; Limbach, H. H.; Martin, G. J.; Martin, M. L.; Schindler, M., Deuterium and Shift Calculation. Springer-Verlag: Berlin ; New York 1991; Vol. 23.
  34. Pettersson, L. G. M.; Wahlgren, U.; Gropen, O., Effective Core Potential Parameters for First- and Second-Row Atoms. *J. Chem. Phys.* **1987**, 86 (4), 2176-2184.
  35. Kuroki, S.; Endo, K.; Maeda, S.; Chong, D. P.; Duffy, P., Analysis of X-Ray Photoelectron Spectra of Silicon-Based Polymers by Demon Density-Functional Calculations Using Model Molecules. *Polym. J.* **1998**, 30, 142.
  36. Venezia, A. M.; Bertoncello, R.; Deganello, G., X-Ray Photoelectron Spectroscopy Investigation of Pumice-Supported Nickel Catalysts. *Surf. Interface Anal.* **1995**, 23 (4), 239-247.
  37. Sirotti, F.; De Santis, M.; Rossi, G., Synchrotron-Radiation Photoemission and X-Ray Absorption of Fe Silicides. *Phys. Rev. B* **1993**, 48 (11), 8299-8306.
  38. Gross, T.; Ramm, M.; Sonntag, H.; Unger, W.; Weijers, H. M.; Adem, E. H., An XPS Analysis of Different  $\text{SiO}_2$  Modifications Employing a C 1s as Well as an Au 4f7/2 Static Charge Reference. *Surf. Interface Anal.* **1992**, 18 (1), 59-64.
  39. Beamson, G.; Briggs, D., *High Resolution XPS of Organic Polymers: The Scienta Esca300 Database* Wiley: New York, 1992; p 295.
  40. Keiji, K.; Jiro, M.; Moritaka, N., Chemical States of Bromine Atoms on  $\text{SiO}_2$  Surface after Hbr Reactive Ion Etching: Analysis of Thin Oxide. *Jpn. J. Appl. Phys.* **1993**, 32 (6S), 3063-3067.
  41. Wertheim, G. K.; Van Attekum, P. T. T. M.; Basu, S., Electronic Structure of Lithium Graphite. *Solid State Commun.* **1980**, 33 (11), 1127-1130.
  42. Larsson, R.; Folkesson, B., The Use of Internal Standards for Measuring the Esca Chemical Shift in Coordination Compounds of Cobalt. *Physica Scripta* **1977**, 16 (5-6), 357-363.
  43. Gelius, U.; Hedén, P. F.; Hedman, J.; Lindberg, B. J.; Manne, R.; Nordberg, R.; Nordling, C.; Siegbahn, K., Molecular

- Spectroscopy by Means of Esca III. Carbon Compounds. *Physica Scripta* **1970**, 2 (1-2), 70-80.
44. Guimon, C.; Gonbeau, D.; Pfister-Guillouzo, G.; Dugne, O.; Guette, A.; Naslain, R.; Lahaye, M., XPS Study of Bn Thin Films Deposited by CVD on SiC Plane Substrates. *Surf. Interface Anal.* **1990**, 16 (1 - 12), 440-445.
45. Bertoncello, R.; Glisenti, A.; Granozzi, G.; Battaglin, G.; Caccavale, F.; Cattaruzza, E.; Mazzoldi, P., Chemical Interactions in Titanium- and Tungsten-Implanted Fused Silica. *J. Non-Cryst. Solids* **1993**, 162 (3), 205-216.
46. Chao, S. S.; Takagi, Y.; Lucovsky, G.; Pai, P.; Custer, R. C.; Tyler, J. E.; Keem, J. E., Chemical States Study of Si in  $\text{SiO}_x$  Films Grown by Pecvd. *Appl. Surf. Sci.* **1986**, 26 (4), 575-583.
47. Chong, D. P., Augmenting Basis Set for Time-Dependent Density Functional Theory Calculation of Excitation Energies: Slater-Type Orbitals for Hydrogen to Krypton *Mol. Phys.* **2005**, 103 (6-8), 749-761.
48. HANDY, N. C.; Cohen, A. J., Left-Right Correlation Energy. *Mol. Phys.* **2001**, 99 (5), 403-412.
49. Lee, C.; Yang, W.; Parr, R. G., Development of the Colle-Salvetti Correlation-Energy Formula into a Functional of the Electron Density. *Phys. Rev. B* **1988**, 37 (2), 785-789.
50. Perdew, J. P.; Burke, K.; Ernzerhof, M., Generalized Gradient Approximation Made Simple. *Phys. Rev. Lett.* **1996**, 77 (18), 3865-3868.
51. Perdew, J. P.; Chevary, J. A.; Vosko, S. H.; Jackson, K. A.; Pederson, M. R.; Singh, D. J.; Fiolhais, C., Atoms, Molecules, Solids, and Surfaces: Applications of the Generalized Gradient Approximation for Exchange and Correlation. *Phys. Rev. B* **1992**, 46 (11), 6671-6687.
52. Van Lenthe, E.; Baerends, E. J., Optimized Slater-Type Basis Sets for the Elements 1-118. *J. Comput. Chem.* **2003**, 24 (9), 1142-1156.
53. ADF. SCM, *Theoretical Chemistry*,. Vrije Universiteit: Amsterdam, The Netherlands, 2016.